

MindScan: Dual Deep Learning system of Brain Tumors Detection and Classification from MRI Scans

BAZGOUR YASSINE¹, ABOUHANE ZAHRA¹, AND QAFFOU ISSAM¹

¹ Semlalia Faculty, Department of Computer Science, Cadi Ayyad University, Marrakesh, Morocco

This project presents MindScan, a web-based hierarchical deep learning system for automated brain tumor detection and classification from MRI images, using MobileNetV2 as the primary model. MRI scans were preprocessed with grayscale conversion, black-border cropping, CLAHE contrast enhancement, bilateral denoising, and intensity normalization to improve feature consistency and generalization. The pipeline employs a dual-stage architecture: a binary classifier detects tumor versus non-tumor cases, followed by a multi-class classifier distinguishing glioma, meningioma, and pituitary tumors. MobileNetV2 trained on preprocessed data achieved 99% validation accuracy for binary classification and 91.3% for multi-class classification. The web interface allows users to upload MRI images and receive real-time predictions, demonstrating reliable performance across diverse tumor types. These results highlight the effectiveness of combining preprocessing, a hierarchical architecture, and a lightweight CNN for accurate, efficient, and accessible brain tumor detection suitable for clinical and real-time applications.

21 B. Aim

22 The primary aim of this project is to develop an intelligent diagnostic system for brain tumor detection and classification using
 23 MRI images. The approach focuses on analyzing high-resolution
 24 brain MRI scans to automatically identify and differentiate be-
 25 tween normal and abnormal cases. The system employs a dual-
 26 structured deep learning architecture, integrating both binary
 27 classification (normal vs. tumor) and multi-class classification
 28 (Glioma, Meningioma, Pituitary) models. This structure enables
 29 the system to first determine the presence of a tumor, and then
 30 accurately classify its specific type, enhancing diagnostic preci-
 31 sion and clinical applicability. Furthermore, the project aims to
 32 integrate this model into a web-based platform called MindScan,
 33 providing an accessible interface for radiologists and healthcare
 34 professionals to facilitate early brain tumor detection, streamline
 35 diagnosis, and support remote medical assessment.
 36

37 C. Related Work

38 Recent research on MRI-based brain tumor analysis focuses
 39 on improving diagnostic accuracy, segmentation quality, and
 40 model reliability. Three representative works illustrate the main
 41 directions in the field.

42 **Explainable ConvMixer-Based Classification Models** Selva
 43 Birunda et al. [1] in 2025 proposed EM-ConvMixer+Net, an
 44 explainable framework combining ConvMixer blocks with atten-
 45 tion mechanisms to improve classification and interpretability.
 46 The model achieves high accuracy and provides visual expla-
 47 nations through Grad-CAM, but its multi-module architecture
 48 increases implementation complexity and computational cost.

49 **YOLO-Based Real-Time Tumor Detection** Nuthi Raju et al.
 50 [2] in 2025 introduced YOLO-Beta11, a lightweight model de-
 51 signed for real-time tumor detection. It integrates attention-
 52 enhanced modules and optimized loss functions, achieving
 53 strong precision and recall while keeping inference efficient.
 54 However, as a single-stage detector, it outputs bounding boxes
 55 rather than detailed tumor masks, limiting its use for tasks re-
 56 quiring pixel-level segmentation.

57 **Hybrid VGG16-InceptionV3 Feature Fusion Models** Jamaa
 58 et al. [3] in 2025 as well, developed a hybrid model that merges
 59 VGG16 and InceptionV3 features for multi-class tumor classifi-
 60 cation. This fusion improves generalization and boosts accuracy
 61 across tumor types. The drawback is the increased model size,
 62 which makes deployment slower and less suitable for resource-
 63 constrained clinical environments.

2

3

4 1. INTRODUCTION

5 A. Problem

6 Brain tumors such as gliomas, meningiomas, and pituitary tu-
 7 mors remain difficult to diagnose early, and they often lead
 8 to severe health outcomes when detected late. Even experi-
 9 enced radiologists can misinterpret MRI scans, especially when
 10 small or subtle abnormalities are present. This challenge is more
 11 pronounced in regions with limited access to specialized radio-
 12 logical expertise, where delays and diagnostic errors are more
 13 common.

14 Traditional diagnosis depends heavily on human interpreta-
 15 tion, which is time-consuming, costly, and prone to subjectivity.
 16 As a result, many patients do not receive timely and accurate
 17 assessments. There is a clear need for intelligent, automated
 18 systems capable of analyzing MRI scans with high precision,
 19 detecting minute patterns that may escape the human eye, and
 20 supporting clinicians in making faster, more reliable decisions.

64 2. METHODOLOGY

65 A. Data

66 A.1. Data Overview

67 The experiments use the Brain Tumor MRI Dataset by Masoud
 68 Nickparvar from Kaggle [4], which includes MRI images la-
 69 beled as glioma, meningioma, pituitary tumor, and no tumor.
 70 Although the dataset provider indicates uniform dimensions,
 71 verification confirmed that all images are consistently sized at
 72 224×224. The original Training and Testing folders were merged
 73 into a single pool, and the final train-validation-test split was
 74 performed programmatically within the code. Since the images
 75 already share the same resolution, only normalization was ap-
 76 plied before feeding them into the models. This setup ensures a
 77 clean, unified dataset suitable for both detection and classifica-
 78 tion tasks.

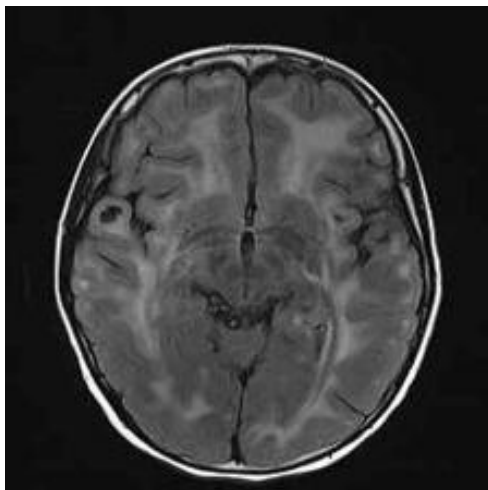


Fig. 1. Normal brain MRI scan with symmetrical structure and no visible abnormal growths or irregularities.

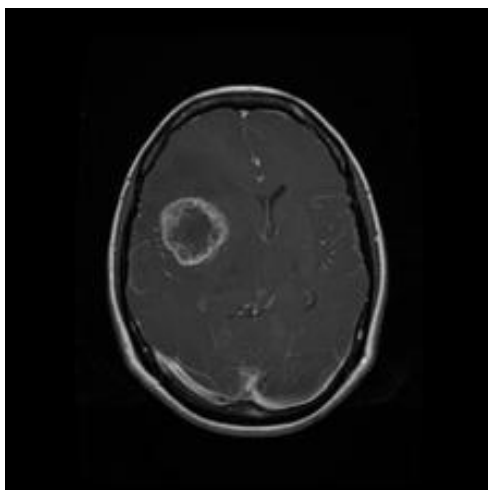


Fig. 2. MRI scan showing an abnormal brain region characterized by irregular mass and tissue deformation, indicative of a brain tumor.

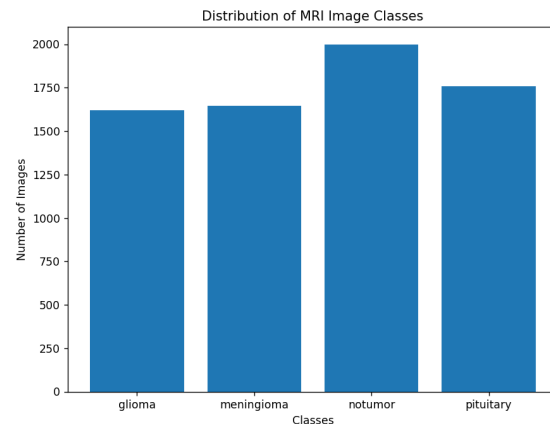


Fig. 3. This graph shows the distribution of the 4 classes, normal and 3 abnormal classes through the dataset

79 A.2. Data Preprocessing

80 The original MRI dataset presents substantial variability in res-
 81 olution, field-of-view, contrast distribution, and noise levels
 82 across subjects and acquisition devices. To obtain standard-
 83 ized, noise-reduced, and contrast-enhanced inputs suitable for
 84 CNN-based tumor classification, we designed a deterministic
 85 preprocessing pipeline applied to every image in dataset. All
 86 steps were implemented in Python using OpenCV.

87 The complete pipeline consists of the following stages:

- 88 1. **Grayscale Loading** All MRI slices were loaded in grayscale
 89 using OpenCV. This ensures a uniform single-channel input
 90 representation across all samples.

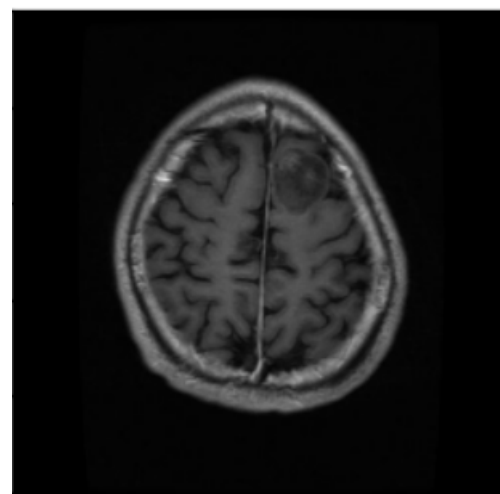


Fig. 4. Original input MRI

- 91 2. **Automatic Black-Border Cropping** Many MRI images con-
 92 tain large black margins surrounding the head. To remove
 93 these regions, we applied a morphological bounding-box
 94 cropping. This step isolates the brain region, reduces irrele-
 95 vant background, and improves consistency across scans.

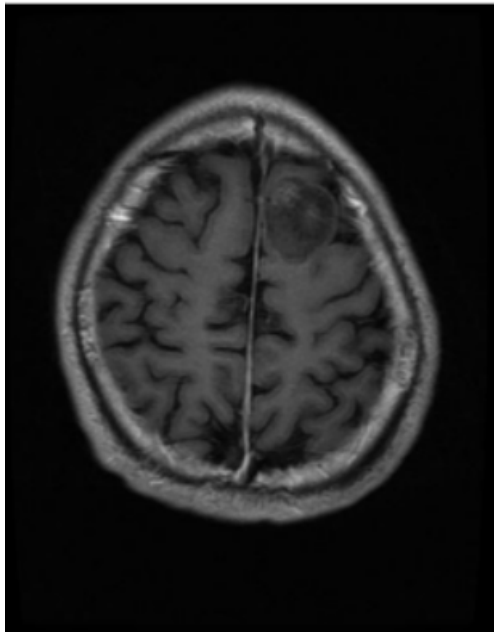


Fig. 5. Output after black-border cropping

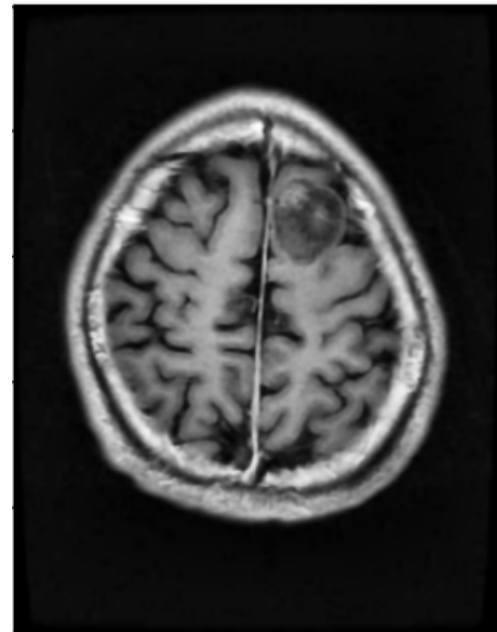


Fig. 7. Output after bilateral filtering

96 3. **Local Contrast Enhancement (CLAHE)** To handle contrast 107
97 heterogeneity between MRI scanners, we applied Contrast 108
98 Limited Adaptive Histogram Equalization (CLAHE) with 109
99 the following parameters: CLAHE locally boosts visibility 110
100 of structures by enhancing edges and intensities without 111
101 amplifying noise excessively. 112

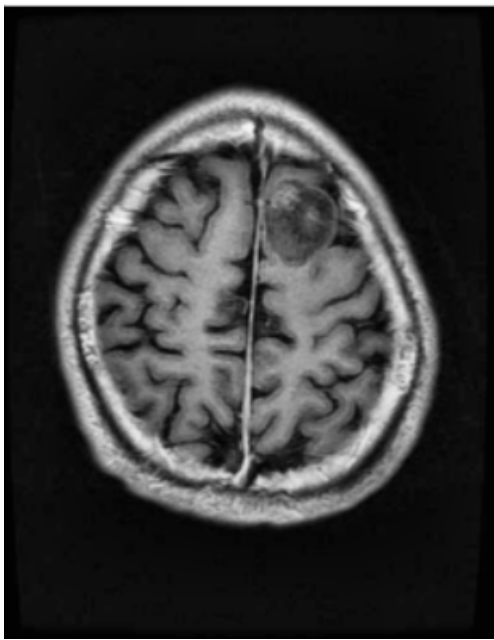


Fig. 6. Output after CLAHE

102 4. **Edge-Preserving Denoising (Bilateral Filter)** Following 103
103 contrast enhancement, residual noise is smoothed using a 104
104 bilateral filter: This filter reduces noise while preserving 105
105 anatomical edges, unlike Gaussian blur which smooths 106
106 edges away. 107

113 5. **Intensity Normalization** Before saving the preprocessed 114
114 images, each image was normalized to the range [0, 1]. This 115
115 normalization ensures stable numerical behavior during 116
116 model training and keeps pixel intensities consistent across 117
117 the dataset. These preprocessed images were then saved 118
118 back as uint8 images (scaled back to 0–255 only for storage), 119
119 while the internal normalized representation is used for 120
120 model input. 121

122 6. **Secondary Normalization (Step 2: Conversion to .npy for 123
123 Training)** A second normalization stage was executed to 124
124 prepare the final model input. 125

A.3. Dataset Configuration for Classification Tasks

126 To prepare the dataset and configurate it for classification task, 127
127 we followed these methods as follow: 128

129 **Tumor vs No-tumor Binary Classification** For implementing 130
130 binary classification we splitted the dataset to contains all 2000 131
131 sample of no tumor class and a chunk of each tumor class, and 132
132 to make the dataset balanced between tumor and no tumor we 133
133 managed to take 667 sample of each three tumor classes which 134
134 resulted of 2001 sample. 135

136 **Three-Class Tumor-Only Classification** To classify tumor 137
137 type, samples from the notumor category are excluded. The 138
138 model learns to discriminate between:

- 139 • glioma
- 140 • meningioma
- 141 • pituitary tumor

142 This configuration focuses strictly on tumors and corresponds to 143
143 clinical tasks requiring tumor-type identification after a positive 144
144 detection. 145

146 **Train, Validation, and Test Split** The binary dataset is then 147
147 split into training, validation, and test sets using a reproducible 148
148 method. 149

random seed. Stratified sampling ensures that both classes maintain the same proportion in all splits. This workflow prevents overfitting, stabilizes learning, and provides a consistent framework for both binary and three-class classification tasks.

B. Models

B.1. Pipeline

The architecture follows a two-stage approach. First, a binary classifier determines whether an MRI scan is abnormal or normal. This step filters out healthy cases, **reducing unnecessary computation for normal images and improving overall detection efficiency**. If the scan is classified as abnormal, it is passed to a multi-class classifier that distinguishes between the specific tumor types—glioma, meningioma, or pituitary tumor. This hierarchical design simplifies the classification task, allows the models to focus on relevant features at each stage, and improves both accuracy and interpretability. [5]

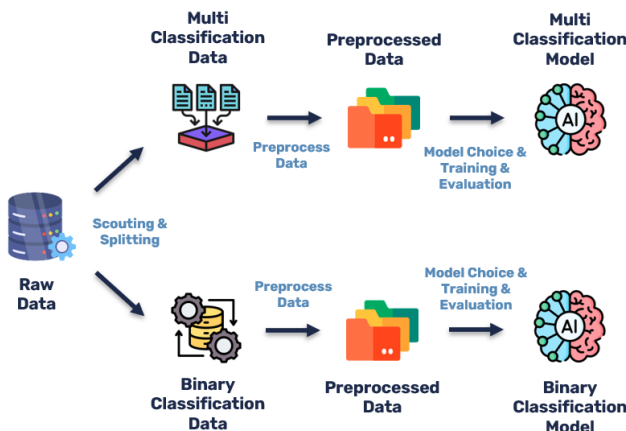


Fig. 8. Pipeline of models

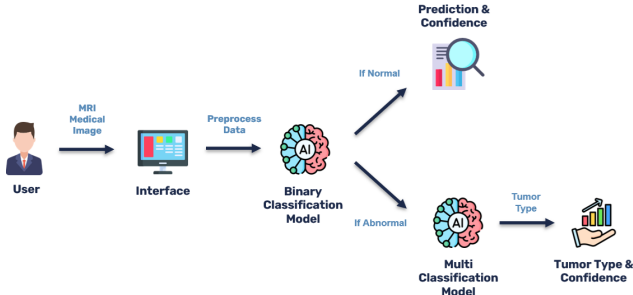


Fig. 9. User scenario

B.2. MobileNetV2

MobileNetV2 is a lightweight convolutional neural network designed for efficient performance on mobile and embedded devices. Introduced by Sandler et al. [6] in 2018, it uses inverted residual blocks with linear bottlenecks, preserving representational power while reducing computation. MobileNetV2 has around 3.4 million parameters and a model size of approximately 14 MB, making it highly compact compared to larger architectures like EfficientNetV2B0. It provides a strong balance of accuracy and speed, supporting real-time inference with low memory and computational requirements. Its main limitation is

that it may not achieve the highest accuracy on very challenging datasets compared to larger models.

B.3. ResNet18

ResNet18 is a convolutional neural network introduced by He et al. [7] in 2016 that employs residual learning to facilitate the training of deeper networks. It consists of 18 layers with skip connections that allow gradients to flow more effectively during backpropagation, addressing the vanishing gradient problem common in deep architectures. ResNet18 has approximately 11.7 million parameters, making it larger than MobileNetV2 but still relatively lightweight compared to deeper ResNet variants. It offers a strong trade-off between accuracy and computational efficiency, making it suitable for tasks requiring reliable feature extraction with moderate resources. Its main limitation is that it may be slower than extremely compact models on mobile or embedded devices.

B.4. EfficientNetV2B0

EfficientNetV2B0 is a state-of-the-art convolutional neural network that employs compound scaling of depth, width, and resolution to optimize accuracy and efficiency. It is designed to achieve high performance with fewer parameters and reduced computational cost compared to traditional large models. The architecture incorporates advanced features such as fused MBConv blocks and progressive learning rate scaling, making it well-suited for a variety of image classification tasks while maintaining a balance between model size, speed, and representational power. [8]

C. Web Interface

The MindScan web interface provides a user-friendly platform for AI-based brain tumor detection. The frontend, built with HTML, CSS, and JavaScript, allows users to upload MRI images and receive predictions instantly. The backend, implemented in Python, processes the images and generates model outputs in real time through a lightweight API. [9], enabling fast, reliable, and accessible brain tumor analysis directly from the browser.

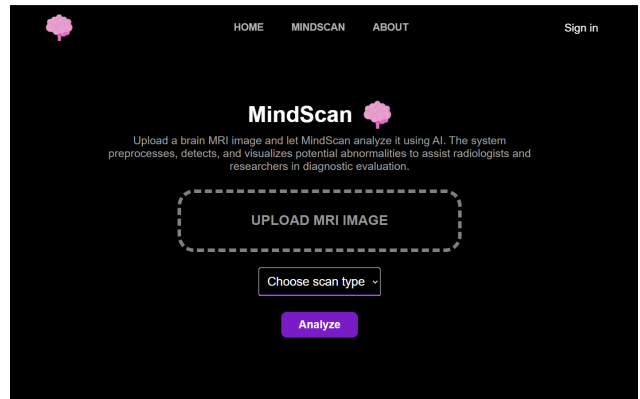


Fig. 10. MindScan interface.

3. RESULTS

A. Binary Classification with MobileNetV2

A.1. Applied on data not preprocessed

We trained MobileNetV2 as a binary classifier to distinguish between normal and abnormal MRI scans. The model achieved rapid convergence, reaching a training accuracy of 99.8% and a

validation accuracy of 98.1% after 10 epochs. F1-score, precision, and recall metrics followed similar trends, with the final validation F1-score reaching 0.981, demonstrating that MobileNetV2 can reliably detect abnormal scans. The training process was stable, with steadily decreasing loss, highlighting the efficiency and suitability of MobileNetV2 for real-time binary classification tasks.

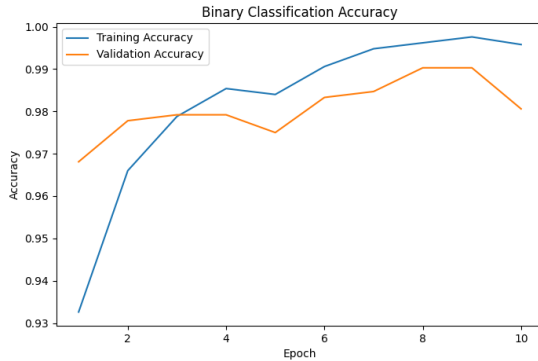


Fig. 11. The curve of the binary classification accuracy

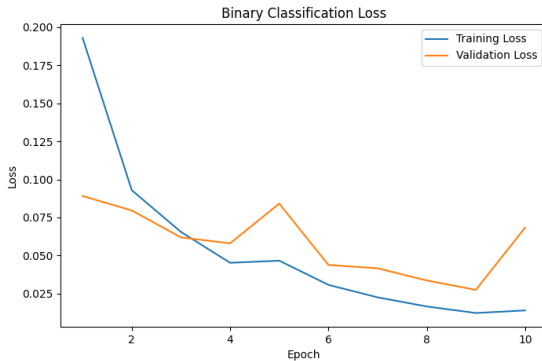


Fig. 12. The curve of the binary classification loss on preprocessed

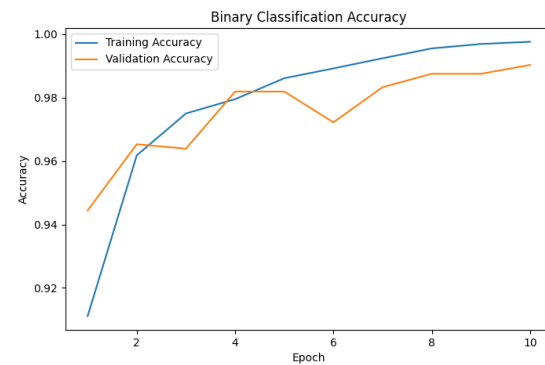


Fig. 13. The curve of the binary classification accuracy on preprocessed data

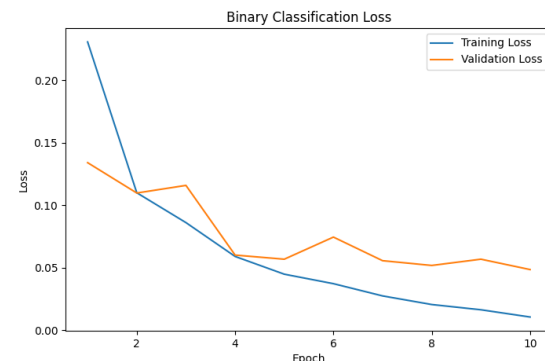


Fig. 14. The curve of the binary classification loss

217 **A.2. Applied on preprocessed data**

218 The model trained on the preprocessed dataset showed a clear
219 improvement in both stability and overall performance. Starting
220 from an initial accuracy of 91%, MobileNetV2 quickly progressed
221 to 99% training accuracy and 99% validation accuracy by the
222 final epoch. Loss values consistently decreased for both training
223 and validation sets, and the high precision, recall, and F1-scores
224 remained closely matched across epochs, indicating balanced
225 predictions with minimal overfitting. Compared to the non-
226 preprocessed experiment, the preprocessed version converged
227 more cleanly, exhibited smoother accuracy and loss curves, and
228 achieved slightly higher final validation performance. These
229 results confirm that preprocessing enhanced feature consistency
230 and helped the model generalize better while maintaining rapid
231 convergence.

232 **B. Multi-Class Classification with MobileNetV2**

233 **B.1. Applied on data not preprocessed**

234 MobileNetV2 was trained to classify abnormal MRI scans into
235 glioma, meningioma, or pituitary tumor categories. The model
236 showed steady improvement over 10 epochs, reaching a training
237 accuracy of 95.4% and a validation accuracy of 87.3%. F1-score,
238 precision, and recall on the validation set were similarly high,
239 indicating that the model reliably distinguishes between different
240 tumor types. The training and validation loss decreased
241 consistently, suggesting effective learning and good generalization,
242 although the validation performance is slightly lower than
243 training, which is expected in multi-class tasks due to higher
244 complexity.

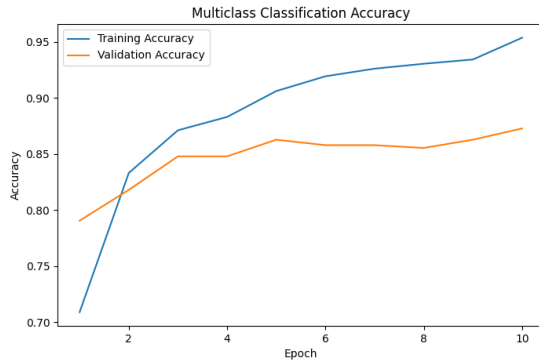


Fig. 15. The curve of the multi-class classification accuracy

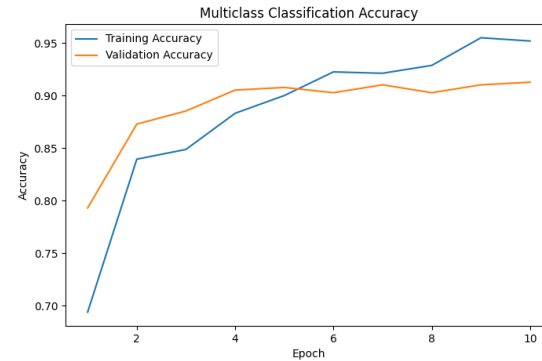


Fig. 17. The curve of the multi-class classification accurac after preprocessing

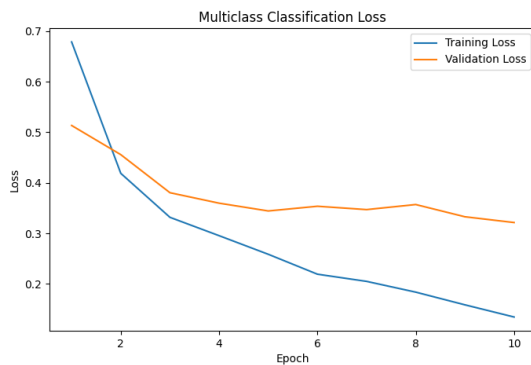


Fig. 16. The curve of the multi-class classification loss

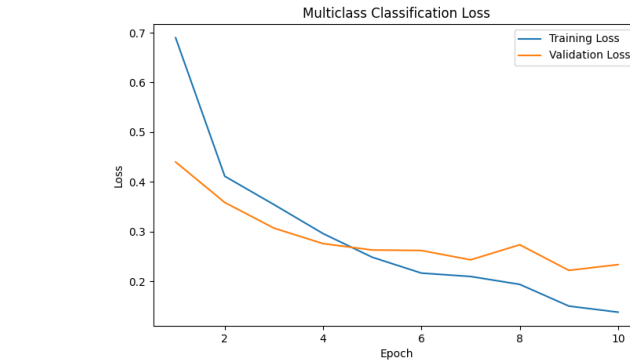


Fig. 18. The curve of the multi-class classification loss after preprocessing

C. Binary Classification with ResNet18

We trained ResNet18 as a binary classifier to distinguish between tumor and non-tumor MRI scans. The model converged quickly, achieving a test accuracy of 98%. Precision, recall, and F1-score metrics indicate strong discriminative ability, with precision for tumor and non-tumor at 1.00 and 0.93, recall at 0.97 and 1.00, and F1-score at 0.98 and 0.97, respectively. However, a noticeable gap between training and validation performance suggests some overfitting, likely due to the relatively small dataset size compared to ResNet18's large capacity. Dropout, early layer freezing, and balanced sampling mitigated overfitting to some extent, but the model's complexity exceeds the amount of available data, limiting generalization in edge cases.

D. Multi Classification with ResNet18

ResNet18 was trained to classify tumor MRI scans into glioma, meningioma, and pituitary tumor categories. The model reached 97% test accuracy, with pituitary tumors identified with near-perfect reliability. Most misclassifications occurred between glioma and meningioma due to their visual similarity. While precision, recall, and F1-score metrics were high across all classes, the large network exhibited signs of overfitting, with training accuracy consistently higher than validation accuracy. Fine-tuning only higher layers, combined with dropout and weight decay, helped control overfitting, but the relatively small dataset limited ResNet18's full generalization potential for multi-class tumor differentiation.

245 B.2. Applied on preprocessed data

246 Training the multiclass classifier on the preprocessed images led
247 to a clear improvement in learning stability and overall perfor-
248 mance. The model began with an accuracy of 69% but quickly
249 progressed, reaching over 90% validation accuracy by the fourth
250 epoch and stabilizing around 91% in the final iteration. Precision,
251 recall, and F1-score followed the same trend, showing consistent
252 and balanced predictions across all tumor categories. The loss
253 steadily decreased for both training and validation sets, and the
254 gap between them remained small, indicating controlled general-
255 ization without overfitting. Compared to the non-preprocessed
256 setup, the preprocessed data enabled smoother convergence
257 and higher final performance, confirming that the preprocessing
258 pipeline strengthened feature quality and improved the model's
259 ability to differentiate between the three tumor types.

285

286 E. Binary Classification with EfficientNetV2B0

287 Training and fine-tuning a large architecture like Efficient
 288 NetV2B0 on a relatively small dataset can easily lead to dramatic
 289 overfitting. The model's high capacity allows it to memorize
 290 training samples rather than generalize to unseen data, which
 291 can significantly reduce its reliability for brain tumor detection
 292 tasks when dataset size is limited.

293 F. Web Interface Demo

294 We conducted tests and demos using the MindScan interface
 295 with sample MRI images randomly from random internet
 296 sources for all tumor classes and no tumor class. The system
 297 successfully analyzed each case, providing accurate predictions
 298 and demonstrating reliable performance across different tumor
 299 types.

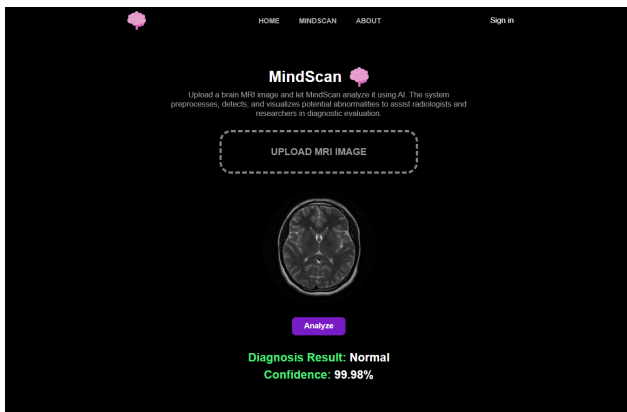


Fig. 19. Test in MindScan interface on a normal sample

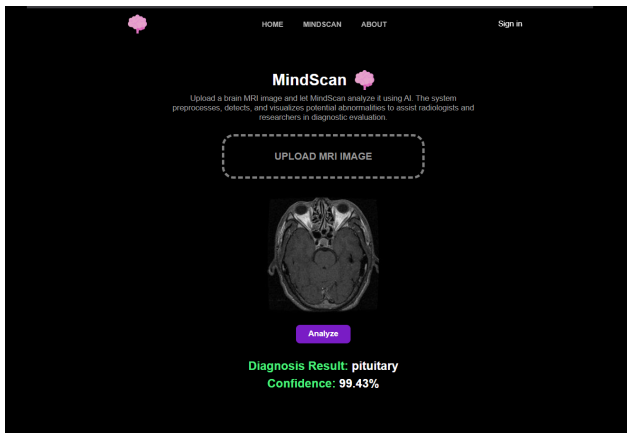


Fig. 20. Test in MindScan interface on an abnormal sample

300 4. DISCUSSION

301 A. MobileNetV2

302 A.1. Applied on data not preprocessed

303 The MobileNetV2-based pipeline performed well for both binary
 304 and multi-class brain tumor classification. Binary classification
 305 achieved near-perfect metrics, while multi-class classification
 306 reached 87.3% validation accuracy, showing reliable tumor type
 307 identification. The hierarchical design proved efficient, and Mo-
 308 bileNetV2's compact size supports fast, web-based deployment.

309 Slight gaps between training and validation suggest that more
 310 data or augmentation could further improve generalization.

311 A.2. Applied on preprocessed data

312 Applying preprocessing led to clear improvements in stability
 313 and overall performance for both binary and multiclass clas-
 314 sification. The binary model reached 99% validation accuracy
 315 with smooth convergence and minimal gaps between training
 316 and validation curves, indicating strong generalization. The
 317 multiclass model also benefited, achieving over 91% validation
 318 accuracy and maintaining consistent precision, recall, and F1-
 319 scores across all classes. Loss decreased steadily in both tasks,
 320 and the training process became more stable compared to the
 321 non-preprocessed setup. These results show that preprocessing
 322 enhanced feature clarity, improved convergence, and strength-
 323 ened MobileNetV2's ability to distinguish brain tumor types.

324 B. Comparison

325 MobileNetV2 trained on preprocessed data demonstrated the
 326 best overall performance for both binary and multi-class brain
 327 tumor classification. The model achieved 99% validation accu-
 328 racy for binary classification and 91.3% for multi-class clas-
 329 sification, with smooth convergence and minimal overfitting.
 330 Preprocessing clearly improved stability, generalization, and
 331 feature consistency, allowing the model to reliably distinguish
 332 tumor types. Its compact size and efficiency also make it ideal
 333 for real-time, web-based deployment, confirming MobileNetV2
 334 on preprocessed data as the optimal choice for this project.

Table 1. Training and Validation Metrics Across Epochs for MobileNetV2 and ResNet18^a

Model / Data	Train Acc	Val Acc	Train Loss	Val Loss
Binary Classification				
MNV2 (Raw)	0.9958	0.9806	0.0139	0.0683
MNV2 (PP)	0.9976	0.9903	0.0105	0.0485
Multi-Class Classification				
MNV2 (Raw)	0.9538	0.8728	0.1346	0.3215
MNV2 (PP)	0.9519	0.9127	0.1377	0.2334

335 ^a Abbreviations: MNV2 = MobileNetV2, PP = Preprocessed, Acc = Accuracy,
 336 Val = Validation.

337 5. LIMITATIONS AND FUTURE WORK

338 Despite the strong performance of MindScan, several limitations exist. The dataset
 339 used is relatively small and sourced from a single public repository, which may
 340 limit the model's generalization to diverse clinical populations. Additionally, the
 341 current system focuses solely on classification and does not provide tumor seg-
 342 mentation, which could be valuable for treatment planning and surgical guidance.
 343 Future work could address these limitations by incorporating larger, multi-center
 344 datasets to improve generalization, adding automated tumor segmentation capa-
 345 bilities, and exploring 3D MRI analysis. Further validation in real-world clinical
 346 settings would also strengthen the system's reliability and applicability.

347 6. CONCLUSION

348 In this work, we developed MindScan, a web-based AI system for brain tumor
 349 detection and classification using MRI images. The proposed hierarchical
 350 approach—binary classification to detect abnormalities followed by multi-class clas-
 351 sification to identify tumor types—demonstrated strong performance, with Mo-
 352 bileNetV2 achieving high accuracy, F1-score, precision, and recall. The system
 353 provides real-time, reliable predictions while remaining lightweight and suitable
 354 for web deployment. These results highlight the potential of AI-assisted tools to

355 support early and accurate diagnosis of brain tumors, improving clinical decision-
356 making and patient outcomes. Future work could focus on expanding the dataset,
357 adding segmentation capabilities, and validating the model across diverse clinical
358 settings.

359 REFERENCES

- 360 1. R. R. S. Selva Birunda, M. Kaliappan, Taylor Francis Online (2025).
<https://doi.org/10.1080/01616412.2025.2574357>.
- 361 2. C. R. B. M. C. Nuthi Raju, Kankanala Srinivas, ScienceDirect (2025).
<https://doi.org/10.1016/j.aej.2025.10.019>.
- 362 3. J. A. . M. A. S. Abdu Alhaji Jamaa, Anum Kamal, Springer Nat. Link
363 (2025). <https://link.springer.com/article/10.1007/s40435-025-01887-0>.
- 364 4. K. M. I. Group, "Brain mri images for brain tumor detection
365 dataset," (2022). <https://www.kaggle.com/datasets/masoudnickparvar/brain-tumor-mri-dataset?resource=download&select=Training>.
- 366 5. DarttGoblin, "Mindscan server repository," https://github.com/DarttGoblin/MindScan_server (2025). Accessed: 2025-12-05.
- 367 6. M. Sandler, A. Howard, M. Zhu, *et al.*, "Mobilenetv2: Inverted residuals
368 and linear bottlenecks," in *Proceedings of the IEEE/CVF Conference on
369 Computer Vision and Pattern Recognition (CVPR)*, (2018), pp. 4510–
370 4520.
- 371 7. K. He, X. Zhang, S. Ren, and J. Sun, "Deep residual learning for image
372 recognition," in *Proceedings of the IEEE Conference on Computer
373 Vision and Pattern Recognition (CVPR)*, (2016), pp. 770–778.
- 374 8. M. Tan and Q. V. Le, "Efficientnetv2: Smaller models and faster training,"
375 in *Proceedings of the International Conference on Machine Learning
376 (ICML)*, (2021), pp. 10096–10106.
- 377 9. DarttGoblin, "Mindscan web interface," <https://darttgoblin.github.io/MindScan/MindScan.html> (2025). Accessed: 2025-12-05.